*Remark 3.28. Scaled Stokes problem.* A scaled Stokes problem of the form

$$\begin{aligned} -\nu\Delta \boldsymbol{u} + \nabla p &= \boldsymbol{f} \text{ in } \Omega, \\ \nabla \cdot \boldsymbol{u} &= 0 \text{ in } \Omega, \end{aligned} \tag{3.37}$$

$\nu > 0$, is sometimes of interest for academic purposes, since in (3.37), the viscous term is scaled in the same form as for the Navier–Stokes equations. Dividing the momentum equation in (3.37) by $\nu$ yields

$$\begin{aligned} -\Delta \boldsymbol{u} + \nabla \left(\frac{p}{\nu}\right) &= \frac{\boldsymbol{f}}{\nu} \text{ in } \Omega, \\ \nabla \cdot \boldsymbol{u} &= 0 \text{ in } \Omega, \end{aligned}$$

which is of the same form as the unscaled version (3.1) with a new pressure and a new source term. Now, the finite element error analysis can be applied in the same way as presented in this section, leading to the estimates of form (3.15), (3.20), (3.21), and (3.24), where the pressure terms are scaled with $\nu^{-1}$. Consequently, one obtains also estimates of the form (3.30) and (3.31) with $\nu^{-1}$ in front of $\|p\|_{H^k(\Omega)}$

$$\begin{aligned} \left\|\nabla(\boldsymbol{u} - \boldsymbol{u}^h)\right\|_{L^2(\Omega)} &\leq Ch^k \left(\|\boldsymbol{u}\|_{H^{k+1}(\Omega)} + \nu^{-1} \|p\|_{H^k(\Omega)}\right), \\ \left\|\nabla \cdot \boldsymbol{u}^h\right\|_{L^2(\Omega)} &\leq Ch^k \left(\|\boldsymbol{u}\|_{H^{k+1}(\Omega)} + \nu^{-1} \|p\|_{H^k(\Omega)}\right). \end{aligned} \tag{3.38}$$

For the estimate of the $L^2(\Omega)$ error of the velocity, one considers again the dual Stokes problem (3.22). Since this problem is formulated with unit viscosity, neither $\boldsymbol{\phi}_{\hat{\boldsymbol{f}}}$ nor $\xi_{\hat{\boldsymbol{f}}}$ nor $\hat{\boldsymbol{f}}$ depend on $\nu$. The error estimate is performed in the same way as in the proof of Theorem 3.23. Instead of (3.27), one obtains

$$\left(\nabla \left(\boldsymbol{u} - \boldsymbol{u}^h\right), \nabla \boldsymbol{\phi}^h\right) = \frac{1}{\nu} \left(\nabla \cdot \boldsymbol{\phi}^h, p - q^h\right) \quad \forall\, q^h \in Q^h.$$

Then, the middle term on the right-hand side of (3.28) is scaled with $\nu^{-1}$ and one gets the scaling $\nu^{-1}$ in (3.29) in front of $\left\|p - q^h\right\|_{L^2(\Omega)}$. Finally, the error estimate

$$\begin{aligned} \left\|\boldsymbol{u} - \boldsymbol{u}^h\right\|_{L^2(\Omega)} \leq\ & Ch^{k+1} \left(\|\boldsymbol{u}\|_{H^{k+1}(\Omega)} + \nu^{-1} \|p\|_{H^k(\Omega)}\right) \\ & \times \left(\left\|\boldsymbol{\phi}_{\hat{\boldsymbol{f}}}\right\|_{H^2(\Omega)} + \left\|\xi_{\hat{\boldsymbol{f}}}\right\|_{H^1(\Omega)}\right) \end{aligned} \tag{3.39}$$

is derived.

Thus, for small values of $\nu$, the term $\nu^{-1} \|p\|_{H^k(\Omega)}$ might dominate the right-hand side of all velocity error bounds.

In estimate (3.32) for the pressure, one has to scale also the term on the left-hand side with $\nu^{-1}$. Rescaling this estimate leads to

$$\left\|p - p^h\right\|_{L^2(\Omega)} \leq Ch^k \left(\nu \left\|\boldsymbol{u}\right\|_{H^{k+1}(\Omega)} + \left\|p\right\|_{H^k(\Omega)}\right). \tag{3.40}$$

□

*Example 3.29. Scaled Stokes problem.* Again, the problem defined in Example 3.26 is considered, see Example 3.27 for the simulations with the unscaled Stokes equations. From the estimates (3.38) and (3.39), one would expect that the velocity errors become large for small $\nu$ and then they scale linearly with $\nu^{-1}$. In contrast, from (3.40) one has the expectation that the pressure error becomes large for large values of $\nu$ and then it scales linearly with $\nu$.

Representative results for the second order Taylor–Hood pair of finite element spaces $P_2/P_1$ on the unstructured grid from Figure 3.2 are presented in Figure 3.7. The dependency of the velocity errors on $\nu^{-1}$ and the pressure error on $\nu$ is clearly visible. On coarse grids, also the linear dependencies on $\nu^{-1}$ and $\nu$, respectively, can be observed. However, one can also see a higher order of decrease for the curves with large errors until they reach the curves for which a dependency on the value of $\nu$ cannot be observed. This decrease is higher by half an order for the velocity errors and by one order for the $L^2(\Omega)$ error of the pressure. To the best of our knowledge, there is no explanation for this behavior so far. □

#### 3.2.1.2 The case $\boldsymbol{V_{\mathrm{div}}^h \subset V_{\mathrm{div}}}$

*Remark 3.30. Pairs of finite element spaces with $V_{\mathrm{div}}^h \subset V_{\mathrm{div}}$.* This section inspects the proofs of the error estimates from Section 3.2.1.1 under the condition that $V_{\mathrm{div}}^h \subset V_{\mathrm{div}}$. It turns out that some terms vanish. An important consequence is that the error estimates for the velocity do not depend any longer on the best approximation errors of the pressure finite element space. In addition, also a scaling of the viscous term as discussed in Remark 3.28 does not influence the velocity error estimates. The estimates in the case $V_{\mathrm{div}}^h \subset V_{\mathrm{div}}$ reflect the physics of the problem properly, in contrast to the estimates for the case $V_{\mathrm{div}}^h \not\subset V_{\mathrm{div}}$, compare Remark 3.8.

The most important pair of conforming inf-sup stable finite element spaces satisfying $V_{\mathrm{div}}^h \subset V_{\mathrm{div}}$ is the Scott–Vogelius pair of finite element spaces $P_k/P_{k-1}^{\mathrm{disc}}$, $k \geq d$, on special grids, see Remarks 2.76 and 2.77. □

**Corollary 3.31. Finite element error estimates for the velocity for inf-sup stable pairs of finite element spaces with $V_{\mathrm{div}}^h \subset V_{\mathrm{div}}$.** *Let the assumptions of Theorem 3.17 be fulfilled and consider an inf-sup stable pair of finite element spaces with $V_{\mathrm{div}}^h \subset V_{\mathrm{div}}$, then*

$$\left\|\nabla(\boldsymbol{u} - \boldsymbol{u}^h)\right\|_{L^2(\Omega)} \leq 2 \inf_{\boldsymbol{v}^h \in V_{\mathrm{div}}^h} \left\|\nabla(\boldsymbol{u} - \boldsymbol{v}^h)\right\|_{L^2(\Omega)} \tag{3.41}$$

*and*

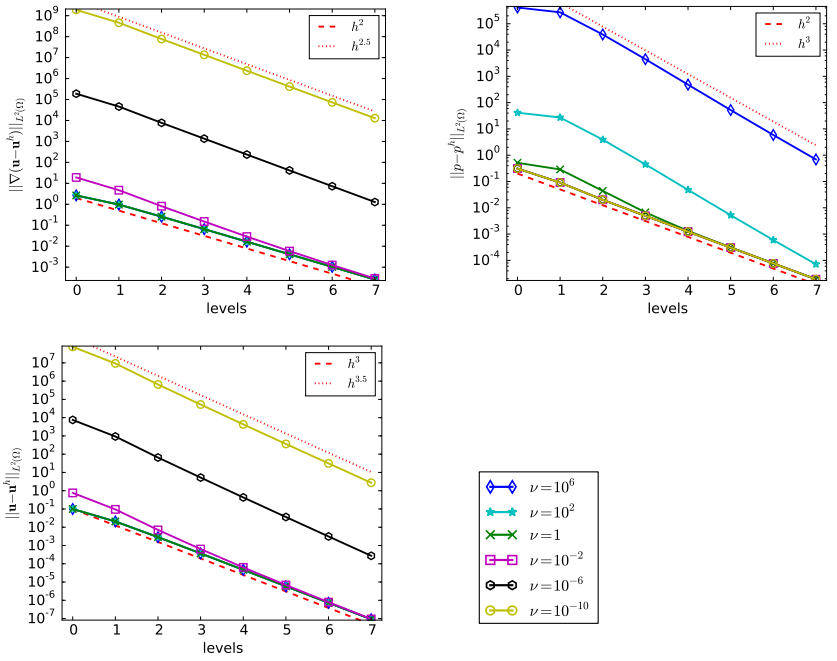


**Fig. 3.7** Example 3.29. Convergence of the errors for the scaled Stokes problem and the $P_2/P_1$ pair of finite element spaces.

$$\left\|\nabla \cdot \boldsymbol{u}^h\right\|_{L^2(\Omega)} = 0. \tag{3.42}$$

*Proof.* The proof of (3.41) is performed in the same way as the proof of Theorem 3.17. Inspecting this proof for pairs of spaces with $V_{\mathrm{div}}^h \subset V_{\mathrm{div}}$, one finds that (3.19) equals zero since $\left\|\nabla \cdot \boldsymbol{\phi}^h\right\|_{L^2(\Omega)} = 0$ for all $\boldsymbol{\phi}^h \in V_{\mathrm{div}}^h$.

Property (3.42) follows directly from the definition of $V_{\mathrm{div}}$. ■

**Corollary 3.32. Finite element error estimate for the $L^2(\Omega)$ norm of the velocity for inf-sup stable pairs of finite element spaces with $V_{\mathrm{div}}^h \subset V_{\mathrm{div}}$.** *Let the assumptions of Theorem 3.23 be fulfilled. If for an inf-sup stable pair of finite element spaces $V_{\mathrm{div}}^h \subset V_{\mathrm{div}}$, then*

$$\begin{aligned}\left\|\boldsymbol{u}-\boldsymbol{u}^h\right\|_{L^2(\Omega)} &\leq \left\|\nabla\left(\boldsymbol{u}-\boldsymbol{u}^h\right)\right\|_{L^2(\Omega)} \\ &\times \sup_{\hat{\boldsymbol{f}}\in L^2(\Omega)} \frac{1}{\left\|\hat{\boldsymbol{f}}\right\|_{L^2(\Omega)}} \inf_{\boldsymbol{\phi}^h\in V_{\mathrm{div}}^h} \left\|\nabla\left(\boldsymbol{\phi}_{\hat{\boldsymbol{f}}}-\boldsymbol{\phi}^h\right)\right\|_{L^2(\Omega)}.\end{aligned} \tag{3.43}$$

*Proof.* The proof proceeds in the same way as the proof of Theorem 3.23. In addition, one can use in (3.28) that $\nabla \cdot \left(\boldsymbol{\phi}^h - \boldsymbol{\phi}_{\hat{\boldsymbol{f}}}\right) = 0$ and $\nabla \cdot \left(\boldsymbol{u}-\boldsymbol{u}^h\right) = 0$ in the weak sense. ■

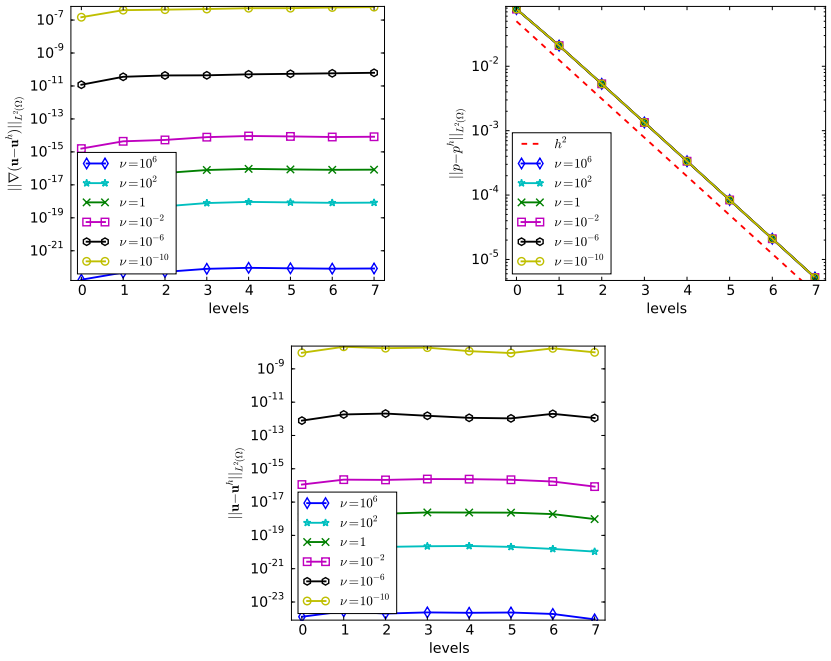


**Fig. 3.8** Example 3.35. Convergence of the errors for the scaled Stokes problem and the $P_2/P_1^{\text{disc}}$ pair of finite element spaces on a barycentric-refined grid.

*Remark 3.33. Pairs of finite element spaces with $V_{\text{div}}^h \subset V_{\text{div}}$.* For pairs of finite element spaces with the property $V_{\text{div}}^h \subset V_{\text{div}}$, it follows from (3.41) and (3.42) that

$$\left\|\nabla(\boldsymbol{u}-\boldsymbol{u}^h)\right\|_{L^2(\Omega)} \leq Ch^k \left\|\boldsymbol{u}\right\|_{H^{k+1}(\Omega)}, \tag{3.44}$$

$$\left\|\nabla\cdot\boldsymbol{u}^h\right\|_{L^2(\Omega)} = 0, \tag{3.45}$$

$$\left\|\boldsymbol{u}-\boldsymbol{u}^h\right\|_{L^2(\Omega)} \leq Ch^{k+1} \left\|\boldsymbol{u}\right\|_{H^{k+1}(\Omega)}. \tag{3.46}$$

These estimates are in particular true for the Scott–Vogelius spaces $P_k/P_{k-1}^{\text{disc}}$, $k \geq d$, on barycentric-refined grids. □

*Remark 3.34. Scaled Stokes problem.* Considering a scaled Stokes problem of the form (3.37), one finds that the scaling $\nu^{-1}$ does not affect the velocity error estimates, in contrast to pairs of finite element spaces with $V_{\text{div}}^h \not\subset V_{\text{div}}$, see Remark 3.28. □

*Example 3.35. The Scott–Vogelius pair of finite element spaces $P_2/P_1^{\text{disc}}$ on a barycentric-refined grid for a no-flow problem.* In this example, the scaled

Stokes problem (3.37) is considered in $\Omega = (0,1)^2$ and with the prescribed solution $\boldsymbol{u} = \mathbf{0}$ and the pressure

$$p(x,y) = 10\left((x-0.5)^3 y + (1-x)^2(y-0.5)^2 - \frac{1}{36}\right).$$

The Scott–Vogelius pair is known to satisfy the discrete inf-sup condition on barycentric-refined grids, see Remark 2.76. The grids were constructed as follows. The unit square was divided into two triangles by connecting the lower left and the upper right corner. This triangulation was uniformly refined once. Then a barycentric-refined grid as depicted in Figure 2.3 was created, giving level 0. After having simulated the problem on this grid, the barycentric refinements were removed, the grid was uniformly refined once more, and again a barycentric refinement was applied, leading to level 1. This process was continued.

The results are presented in Figure 3.8. The velocity error is always a small constant, independently of the value of $\nu$. The increase of this constant is due to the increase of the condition number of the linear saddle point problems for small $\nu$. Hence, this increase reflects round-off errors of the solver. Since the first term on the right-hand side of estimate (3.40) vanishes, one expects that the pressure error in $L^2(\Omega)$ is independent of $\nu$, which can be observed very well in the computational results.

As comparison, results obtained with the Taylor–Hood finite element $P_2/P_1$ computed on the irregular grid from Figure 3.2 are depicted in Figure 3.9. Even for moderate values of $\nu$, the discrete velocity field is far away from being a no-flow field. The dependency of the velocity errors on the viscosity can be clearly observed in this simple example. This result reflects once more the potential impact of the pressure on the error of the velocity for pairs of spaces that do not satisfy $V_{\mathrm{div}}^h \subset V_{\mathrm{div}}$. Note that the order of convergence of both velocity errors is higher by 0.5 than predicted by the analysis. □

## 3.3 Stabilized Finite Element Methods Circumventing the Discrete Inf-Sup Condition

*Remark 3.36. Motivation.* The application of inf-sup stable pairs of finite elements requires the use of different spaces for velocity and pressure. Moreover, it is not possible to use conforming spaces of lowest order for the discrete velocity, i.e., $P_1$ or $Q_1$ finite element spaces. However, software for solving incompressible flow problems contains often just one finite element space and then usually $P_1$ or $Q_1$. In such situations, it is necessary to modify the discrete problem such that the satisfaction of the discrete inf-sup condition (2.32) is not longer necessary. To this end, one has to remove the saddle point struc-

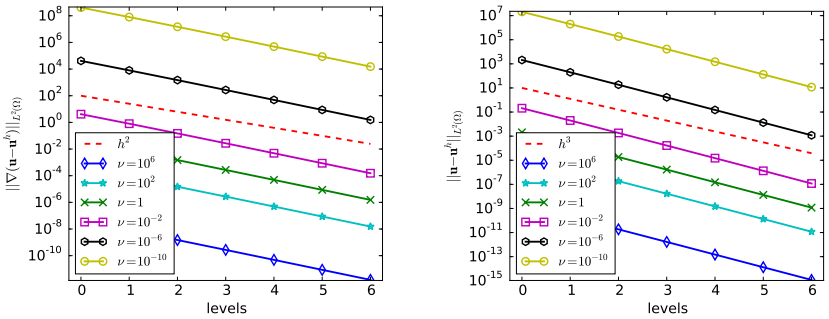


**Fig. 3.9** Example 3.35. Convergence of the velocity errors for the scaled Stokes problem and the $P_2/P_1$ pair of finite element spaces.

ture of the discrete problem, i.e., one has to remove the zero matrix block in the pressure-pressure coupling of the saddle point problem.

There are several proposals in the literature for defining appropriate pressure-pressure couplings, so-called stabilization terms. One class are so-called pseudo-compressibility methods. The strong form of such methods might look as follows:

- Pressure Stabilization Petrov–Galerkin (PSPG) method

$$-\nabla \cdot \boldsymbol{u} + \delta \Delta p = 0,$$

- penalty method

$$-\nabla \cdot \boldsymbol{u} - \delta p = 0,$$

- artificial compressibility method

$$-\nabla \cdot \boldsymbol{u} - \delta \partial_t p = 0,$$

where $\delta$ is some parameter which has to be chosen appropriately.

Note that the introduction of a pressure-pressure coupling perturbs the continuity equation and thus the conservation of mass. In addition, each stabilization term contains parameters. The asymptotic optimal choice of stabilization parameters can be determined often with results from numerical analysis, e.g., with conditions for the existence and uniqueness of a solution of the stabilized problem or from optimal error estimates. However, the user still has to choose concrete parameters in simulations and, depending on the parameter, different concrete choices of the same asymptotic type might sometimes lead to rather different numerical solutions.

Detailed information on pressure-stabilized methods can be found in the recent review paper John *et al.* (2020). □